IMAGING IN NEURAL REGENERATION

Ultrasound imaging of chitosan nerve conduits that bridge sciatic nerve defects in rats

The repair of peripheral nerve injuries with autologous nerve remains the gold standard (Wang et al., 2005; Yao et al., 2010; Deal et al., 2012; Kriebel et al., 2014; Liu et al., 2014; Tamaki et al., 2014; Yu et al., 2014; Zhu and Lou, 2014). With advances in tissue engineering and biomaterials, tissue-engineered nerve conduits with various biomaterials and structures, such as collagen and chitosan nerve conduits, have already been used in the clinic as alternatives to autologous nerve in the repair of peripheral nerve injury (Wang et al., 2012; Svíženská et al., 2013; Eppenberger et al., 2014; Gu et al., 2014; Koudehi et al., 2014; Moya-Díaz et al., 2014; Novajra et al., 2014; Okamoto et al., 2014; Shea et al., 2014; Singh et al., 2014; Tamaki et al., 2014; Yu et al., 2014). Therefore, new simple and effective methods are needed to better evaluate the outcomes of repair using nerve conduits *in vivo*. Ultrasound is a common noninvasive clinical detection modality that has been used in many fields. However, ultrasound has only rarely been used to observe implanted nerve conduits *in vivo*. Haug et al. (2013) tried to displace the collagen nerve conduit for repairing the digital nerve under ultrasound. Here, we report the first use of ultrasound to noninvasively observe the changes in chitosan nerve conduits implanted in rats over time.

Chitosan (Nantong Xincheng Biochemical Company, Nantong, Jiangsu Province, China) was purified twice by dissolution in 10 g of acetic acid, filtration, precipitation with 50 g of NaOH, and finally drying in a vacuum at room temperature. The degree of chitosan deacetylation was 92.3% as measured by titration. After 5 g of chitosan had completely dissolved in 100 mL of 0.15 mol/L hydrochloric acid, 10% gelatin and then 5 g of chitin powder were added while stirring, forming an opaque viscous liquid. The chitin/chitosan mixture was then injected into stainless-steel casting molds, which were then sealed and placed at −12°C for 2–4 hours. The frozen gels were removed and soaked in 4 mol/L NaOH for 4 hours to neutralize any remaining lactic acid and to complete solidification. The conduits were rinsed repeatedly with distilled water to remove any residual NaOH and sodium lactate and lyophilized under a 35–45 mTorr vacuum for 20 hours. The resulting porous conduits were 2 mm inner diameter, 3 mm outer diameter, and 80 mm long (Yang et al., 2011).

A total of 21 clean, female, 2-month-old Sprague-Dawley rats were provided by the Experimental Animal Center of Nantong University, China (license No. SCXK (Su) 2008-0010). The animals were housed in a temperature-controlled environment and allowed food and water *ad libitum*. All experimental protocols were approved by the Administration Committee of Experimental Animals, Jiangsu Province, China, in accordance with the guidelines of the Institutional Animal Care and Use Committee, Nantong University, China. The rats were deeply anesthetized with an intraperitoneal injection of a compound anesthetic (chloral hydrate: 4.25 g, magnesium sulfate: 2.12 g, sodium pentobarbital: 886 mg, ethanol: 14.25 mL, and propylene glycol: 33.8 mL in 100 mL) at a dose of 0.2–0.3 mL/100 g. The skin and muscle were incised to expose the sciatic nerve at the left mid-thigh. An 8-mm segment of the sciatic nerve (from about 10 mm distal to the proximal end to the ischial tuberosity) was resected to produce a 10-mm gap after slight retraction of the distal and proximal stumps. The nerve gap was bridged by a chitosan nerve conduit, and the proximal and distal nerve stumps were inserted into the two ends of the conduit (1 mm was inserted for each end). Then, the muscle layers were closed with sutures, and the skin was closed with wound clips. After surgery, the animals were placed in warmed cages (Yang et al., 2011).

At 1, 2, 3, 4, 8, 12, and 24 weeks after surgery ($n = 3$ in each group), the rats were again deeply anesthetized with the compound anesthetic. A B-mode ultrasound (HIVISION Avius, HITACHI, Chiba Kashiwa, Japan) equipped with a high-resolution linear transducer with a frequency range of 7.5 to 10 MHz and a gel pad serving as an interface between the transducer and fur was used to detect the nerve conduit implanted in the rat. After ultrasound imaging, the surgical site at the left mid-thigh was reopened to expose the nerve conduit. The length and outer diameter were measured with a ruler after photographing the nerve conduit. The ultrasound imaging clearly showed the longitudinal section, as well as the distal and proximal nerves and cross section of the nerve conduit surrounded by muscles (**Figure 1**). The length and outer diameter of the nerve conduit measured by ultrasound were not different ($P > 0.05$) than those measured by ruler after dissection at the different time points (**Figure 2**).

In addition, decreases in both the length and outer diameter were seen from 12 to 24 weeks. The decrease in length ($P < 0.05$) from 12 to 24 weeks was more evident, and this difference reflected the degradation mode of the nerve conduit *in vivo* in rat. There was no evident fracture or collapse of the nerve conduit. However, the two ends of the nerve conduit had clearly shortened at 24 weeks, and a moderate collapse of the cross section was also observed at 24 weeks (**Figures 1 and 2**).

The strain ratio of the nerve conduit was also measured with ultrasound, which reflects the elasticity of the nerve conduit wall. The gradual increase in the strain ratio of the nerve conduit over time suggests that the nerve conduit degraded *in vivo* (**Figure 3**).

Based on these results, the morphological changes of the nerve conduit can be observed by ultrasound imaging *in vivo*. In addition, the strain ratio measured by ultrasound may be an objective reflection of the degradation of the nerve conduit *in vivo*. Moreover, any unsatisfactory complications after implantation, such as fracture, collapse, bleeding, or unusual swelling of the nerve conduits, may be easily identified.

However, some factors are related to the effect of ultrasound detection closely. A specialized training is necessary to identify the peripheral nerve and nerve conduit for the ultrasound detector. The image resolution is relative to the ultrasound frequency. Different frequencies maybe suitable for different conduits made of different biomaterials. Because the rat was small on volume, which has a limited absorption capacity of biomaterials, the degradation of chitosan *in vivo* seemed relatively slow. Also we attempted to detect the dog, a bigger animal, with ultrasound and the trend of degradation of conduit was earlier and more evident.

Ultrasound, as a noninvasive imaging modality, can be used as a supplementary observation method during conventional animal experiments on peripheral nerve tissue engineering.

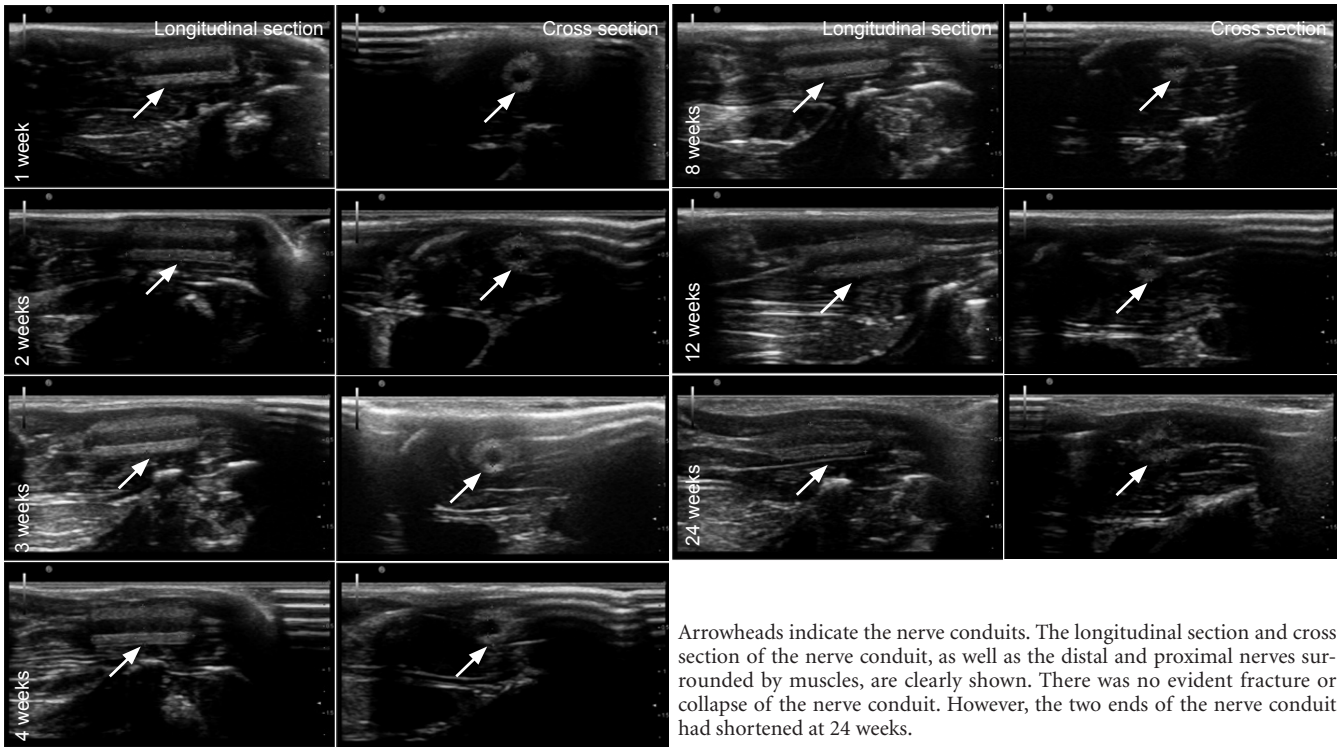

Arrowheads indicate the nerve conduits. The longitudinal section and cross section of the nerve conduit, as well as the distal and proximal nerves surrounded by muscles, are clearly shown. There was no evident fracture or collapse of the nerve conduit. However, the two ends of the nerve conduit had shortened at 24 weeks.

Figure 1 Ultrasound imaging of the morphology of a chitosan nerve conduit in a rat model of sciatic nerve defects after implantation.

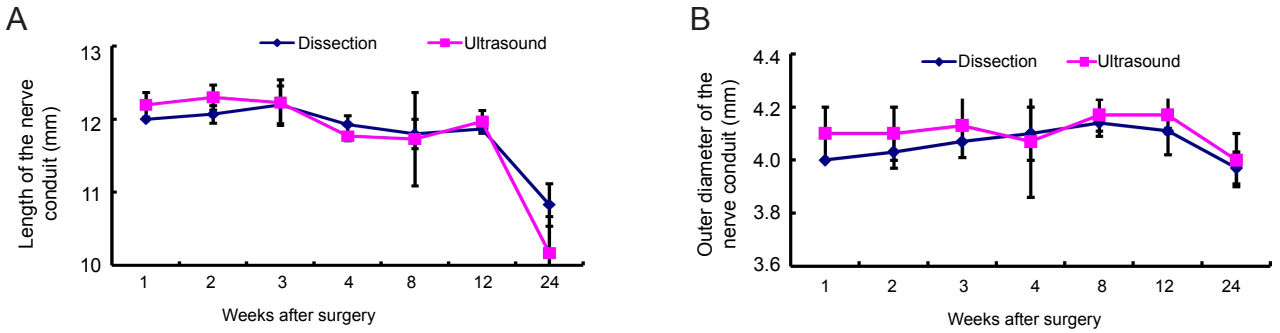

Figure 2 Length (A) and outer diameter (B) of the nerve conduit measured by ultrasound and with a ruler after dissection.
The data are shown as mean ± SEM. Differences between groups at the same times after surgery were analyzed using unpaired Student's *t*-tests. Differences between different time points in the same group after surgery were analyzed using one-way analysis of variance.

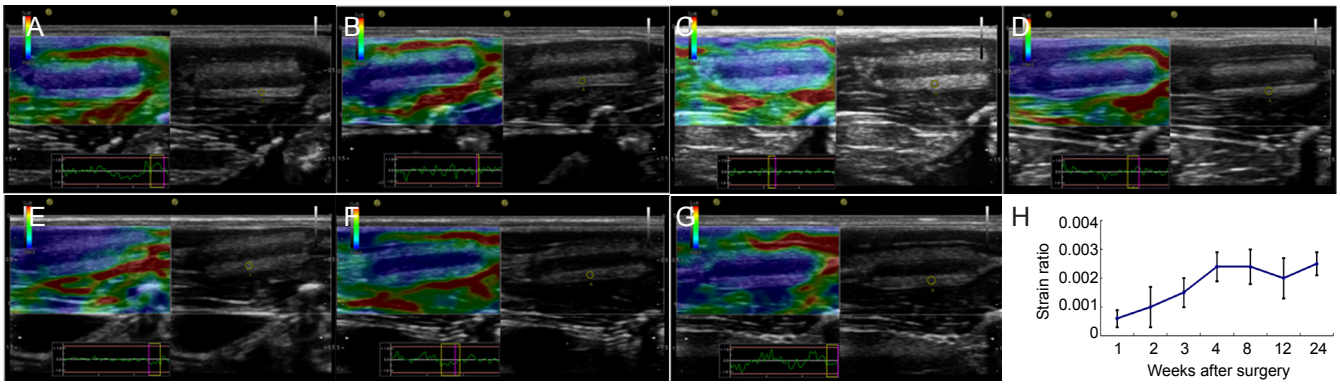

Figure 3 Ultrasound imaging of the elasticity of the chitosan nerve conduit in a rat model of sciatic nerve defects after implantation.
The elasticity and hardness of nerve conduits are shown at 1 (A), 2 (B), 3 (C), 4 (D), 8 (E), 12 (F), and 24 weeks (G) after surgery. Red indicates softer regions and blue indicates harder. In the images, a few colors indicate different degrees of tissue deformation under pressure. Complete deformation is shown as uniform green. The majority of deformations were mostly green with small blue areas. Small deformation is shown as blue in the center surrounded by a small area of green. No deformation is shown as uniform blue. (H) Strain ratio of the nerve conduit over time. The data are shown as mean ± SEM.

Xiaoyang Chen[2], Yifei Yin[2], Tingting Zhang[2], Yahong Zhao[3], Yumin Yang[3], Xiaomei Yu[2], Hongkui Wang[1, 3]
1 School of Biology and Basic Medical Sciences, Soochow University, Suzhou, Jiangsu Province, China
2 Department of Doppler Ultrasound, Affiliated Hospital of Nantong University, Nantong, Jiangsu Province, China
3 Jiangsu Key Laboratory of Neuroregeneration, Nantong University, Nantong, Jiangsu Province, China

Xiaoyang Chen and Yifei Yin contributed equally to this work.
***Corresponding author**: Hongkui Wang, School of Biology and Basic Medical Sciences, Soochow University, Suzhou 215123, Jiangsu Province, China; Jiangsu Key Laboratory of Neuroregeneration, Nantong University, Nantong, Jiangsu Province, China, wang-hongkui@ntu.edu.cn.*
***Funding:** The research is supported by the National High Technology Research and Development Program of China, No. 2012AA020502; the National Natural Science Foundation of China, No. 81171457 and 81371687; and the Priority of Academic Program Development of Jiangsu Higher Education Institutions.*
***Author contributions:** Yang YM checked and revised this article. Wang HK designed and evaluated this study, and wrote the manuscript. Chen XY and Yin YF designed and performed the experiments. Zhang TT and Zhao YH performed the experiments. Yu XM collected the data. All authors approved the final version of the paper.*
***Conflicts of interest:** None declared.*
***doi:**10.4103/1673-5374.137592 **http:**//www.nrronline.org/*
***Accepted:** 2014-06-06*

Chen XY, Yin YF, Zhang TT, Zhao YH, Yang YM, Yu XM, Wang HK. Ultrasound imaging of chitosan nerve conduits that bridge sciatic nerve defects in rats. Neural Regen Res. 2014;9(14):1386-1388.

References

Deal DN, Griffin JW, Hogan MV (2012) Nerve conduits for nerve repair or reconstruction. J Am Acad Orthop Surg 20:63-68.
Eppenberger P, Andreisek G, Chhabra A (2014) Magnetic resonance neurography: diffusion tensor imaging and future directions. Neuroimag Clin N Am 24:245-256.
Gu Y, Zhu J, Xue C, Li Z, Ding F, Yang Y, Gu X (2014) Chitosan/silk fibroin-based, Schwann cell-derived extracellular matrix-modified scaffolds for bridging rat sciatic nerve gaps. Biomaterials 35:2253-2263.
Haug A, Bartels A, Kotas J, Kunesch E (2013) Sensory recovery 1 year after bridging digital nerve defects with collagen tubes. J Hand Surg Am 38:90-97.
Koudehi MF, Fooladi AA, Mansoori K, Jamalpoor Z, Amiri A, Nourani MR (2014) Preparation and evaluation of novel nano-bioglass/gelatin conduit for peripheral nerve regeneration. J Mater Sci Mater Med 25:363-373.
Kriebel A, Rumman M, Scheld M, Hodde D, Brook G, Mey J (2014) Three-dimensional configuration of orientated fibers as guidance structures for cell migration and axonal growth. J Biomed Mater Res B Appl Biomater 102:356-365.
Liu R, Qin J, Zhao L, Zhang X, Xue X (2014) The microstructures and materials of nerve conduits used in peripheral nerve regeneration. J Biomater Tissue Eng 4:65-83.
Mohammadi R, Sanaei N, Ahsan S, Rostami H, Abbasipour-Dalivand S, Amini K (2014) Repair of nerve defect with chitosan graft supplemented by uncultured characterized stromal vascular fraction in streptozotocin induced diabetic rats. Int J Surg 12:33-40.
Moya-Díaz J, Peña OA, Sánchez M, Ureta DA, Reynaert NG, Anguita-Salinas C, Marín G, Allende ML (2014) Electroablation: a method for neurectomy and localized tissue injury. BMC Dev Biol 14:7.
Novajra G, Tonda-Turo C, Vitale-Brovarone C, Ciardelli G, Geuna S, Raimondo S (2014) Novel systems for tailored neurotrophic factor release based on hydrogel and resorbable glass hollow fibers. Mater Sci Eng C Mater Biol Appl 36:25-32.
Okamoto M, Tanaka H, Okada K, Kuroda Y, Nishimoto S, Murase T, Yoshikawa H (2014) Methylcobalamin promotes proliferation and migration and inhibits apoptosis of C2C12 cells via the Erk1/2 signaling pathway. Biochem Biophys Res Commun 443:871-875.
Shea JE, Garlick JW, Salama ME, Mendenhall SD, Moran LA, Agarwal JP (2014) Side-to-side nerve bridges reduce muscle atrophy after peripheral nerve injury in a rodent model. J Surg Res 187:350-358.
Singh B, Singh V, Krishnan A, Koshy K, Martinez JA, Cheng C, Almquist C, Zochodne DW (2014) Regeneration of diabetic axons is enhanced by selective knockdown of the PTEN gene. Brain 137:1051-1067.
Speck AE, Ilha J, do Espírito Santo CC, Aguiar AS, dos Santos AR, Swarowsky A (2014) The IBB forelimb scale as a tool to assess functional recovery after peripheral nerve injury in mice. J Neurosci Methods 226:66-72.
Svíženská IH, Brázda V, Klusáková I, Dubový P (2013) Bilateral changes of cannabinoid receptor type 2 protein and mRNA in the dorsal root ganglia of a rat neuropathic pain model. J Histochem Cytochem 61:529-547.
Tamaki T, Hirata M, Soeda S, Nakajima N, Saito K, Nakazato K, Okada Y, Hashimoto H, Uchiyama Y, Mochida J (2014) Preferential and comprehensive reconstitution of severely damaged sciatic nerve using murine skeletal muscle-derived multipotent stem cells. PLoS One 9:e91257.
Tseng TC, Hsu SH (2014) Substrate-mediated nanoparticle/gene delivery to MSC spheroids and their applications in peripheral nerve regeneration. Biomaterials 35:2630-2641.
Wang H, Zhao Q, Zhao W, Liu Q, Gu X, Yang Y (2012) Repairing rat sciatic nerve injury by a nerve-growth-factor-loaded, chitosan-based nerve conduit. Biotechnol Appl Biochem 59:388-394.
Wang L, Rouleau DM, Beaumont E (2013) Most effective adjuvant treatments after surgery in peripheral nerve laceration: Systematic review of the literature on rodent models. Restor Neurol Neuros 31:253-262.
Wang R, Rossomando A, Sah DWY, Ossipov MH, King T, Porreca F (2014) Artemin induced functional recovery and reinnervation after partial nerve injury. Pain 155:476-484.
Wang X, Hu W, Cao Y, Yao J, Wu J, Gu X (2005) Dog sciatic nerve regeneration across a 30-mm defect bridged by a chitosan/PGA artificial nerve graft. Brain 128:1897-1910.
Yang Y, Yuan X, Ding F, Yao D, Gu Y, Liu J, Gu X (2011) Repair of rat sciatic nerve gap by a silk fibroin-based scaffold added with bone marrow mesenchymal stem cells. Tissue Eng Part A 17:2231-2244.
Yao L, de Ruiter GCW, Wang H, Knight AM, Spinner RJ, Yaszemski MJ, Windebank AJ, Pandit A (2010) Controlling dispersion of axonal regeneration using a multichannel collagen nerve conduit. Biomaterials 31:5789-5797.
Yu W, Jiang X, Cai M, Zhao W, Ye D, Zhou Y, Zhu C, Zhang X, Lu X, Zhang Z (2014) A novel electrospun nerve conduit enhanced by carbon nanotubes for peripheral nerve regeneration. Nanotechnology 25:165102.
Zhang RX, Zhang FF, Li XB, Huang SX, Zi XH, Liu T, Liu SM, Li XN, Xia K, Pan Q, Tang BS (2014) A novel transgenic mouse model of Chinese Charcot-Marie-Tooth disease type 2L. Neural Regen Res 9:413-419.
Zhu G, Lou W (2014) Regeneration of facial nerve defects with xenogeneic acellular nerve grafts in a rat model. Head Neck 36:481-486.

Copyedited by McCarty W, Stow A, Yu J, Qiu Y, Li CH, Song LP, Zhao M